GEOMETRICAL STIFFNESS OF THIN-WALLED I-BEAM ELEMENT BASED ON RIGID-BEAM ASSEMBLAGE CONCEPT

J. D. Yau [*]

Department of Architecture
Department of Transportation Management
Tamkang University
New Taipei City, Taiwan 25137, R.O.C.

S.-R. Kuo

Department of Harbor and River Engineering
National Taiwan Ocean University
Keelung, Taiwan 20224, R.O.C.

ABSTRACT

Using conventional virtual work method to derive geometric stiffness of a thin-walled beam element, researchers usually have to deal with nonlinear strains with high order terms and the induced moments caused by cross sectional stress results under rotations. To simplify the laborious procedure, this study decomposes an I-beam element into three narrow beam components in conjunction with geometrical hypothesis of rigid cross section. Then let us adopt Yang *et al*.'s simplified geometric stiffness matrix $[k_g]_{12 \times 12}$ of a rigid beam element as the basis of geometric stiffness of a narrow beam element. Finally, we can use rigid beam assemblage and stiffness transformation procedure to derivate the geometric stiffness matrix $[k_g]_{14 \times 14}$ of an I-beam element, in which two nodal warping deformations are included. From the derived $[k_g]_{14 \times 14}$ matrix, it can take into account the nature of various rotational moments, such as semi-tangential (ST) property for St. Venant torque and quasi-tangential (QT) property for both bending moment and warping torque. The applicability of the proposed $[k_g]_{14 \times 14}$ matrix to buckling problem and geometric nonlinear analysis of loaded I-shaped beam structures will be verified and compared with the results presented in existing literatures. Moreover, the post-buckling behavior of a centrally-load web-tapered I-beam with warping restraints will be investigated as well.

Keywords: Geometric nonlinear analysis, Rigid beam, Thin-walled beam, Warping.

1. INTRODUCTION

Because of high load-carrying capacity within elastic range, thin-walled beam structures are usually used in civil engineering. Over the past several decades, numerous researchers have dedicated their contributions to fundamental buckling theory of thin-walled beams in an analytical way [1-9]. With the force equilibrium described in buckled positions, the governing equations and critical loads of elastic lateral buckling analysis of I-shaped beams were conducted and solved in references [2-5]. According to theoretical investigations and experimental demonstrations, Kitipornchai and Trahair [6-8] indicated that the web-tapering effect of torsion and the second order effect of a central load above the beam axis would reduce the lateral buckling strength of tapered I-beams significantly.

With the advent of high-speed digital computers, finite element methods provided an efficient tool for response prediction of complicated structures and reasonable simulation of real behaviors of original structures [10]. Including the rotational properties of moments, Yang and McGuire [11,12] adopted virtual work method to derive a bisymmetric thin-walled open

cross section beam element and performed a series of geometric nonlinear analysis of I-beam structures. In recent years, Yang *et al*. [13-17] proposed a rigid body qualified stiffness equation for a three dimensional (3D) solid beam that warping deformation was not taken into account to carry out buckling and geometric nonlinear analyses of framed structures. Their studies indicated that the rigid body qualified geometric stiffness matrix $[k_g]_{12 \times 12}$ is accurate and efficient in simulating the large-displacement nonlinear analysis of framed structures [15-17]. In this paper, Yang's rigid body qualified geometric stiffness matrix is denoted as $[k_g]_{12 \times 12}$. Concerning the vibration and large deformation behaviors of thin-walled beam structures, useful research works are available in references [18-23,30,31].

However, Using conventional virtual work method to derive geometric stiffness of a thin-walled beam element, researchers usually have to deal with nonlinear strains with high order terms and the *induced moments* caused by cross sectional stress results under rotations. [24,25], in which nonlinear strain components involving bending, warping, and torsional deformations [33] have to be considered. To circumvent the complicated

---

[*] corresponding author (jdyau@mail.tku.edu.tw)

procedure, this paper regarded an I-beam element as an assemblage of three narrow beams, *i.e.*, two flanges and one web so that the geometric stiffness matrix of each of the beams can be represented by the simplified $[k_g]_{12 \times 12}$ matrix derived from Yang *et al*'s rigid beam theory [17]. Based on the geometrical hypothesis of rigid cross section, the geometric stiffness matrix $[k_g]_{14 \times 14}$ including warping deformations of a thin-walled I-beam element is achieved by assembling all the geometric stiffness matrices of the three sub-beam elements through stiffness transformation procedure [28]. In this paper, $[k_g]_{14 \times 14}$ matrix represents the geometric stiffness matrix of a thin-walled I-beam element including warping deformations, in which the properties of moments under rotations are taken into account, such as semi-tangential (ST) property for St. Venant torque and quasi-tangential (QT) property for both bending moment and warping torque. To demonstrate the accuracy of the proposed $[k_g]_{14 \times 14}$ matrix for thin-walled I-beam structures in numerical computations, the buckling and geometrical nonlinear analyses of loaded I-beam structures are computed and compared with those given in existing literatures.

2. THEORETICAL FORMULATION

Prior to deriving the $[k_g]_{14 \times 14}$ matrix of an I-beam element, basic assumptions are given as follows [3]: (1) The material is linear elastic, isotropic and homogeneous; (2) The dimensions of cross section are small compared with the beam length, and the I-beam is bi-symmetric and perfectly straight; (3) During deformation, every cross section of the I-beam remains *rigid* in its own plane while free to warp in its out-of plane so that the effects of local buckling and shape-distortion can be neglected; (4) The twisting angle about the centroidal axis of I-section is reasonably small in an incremental step; (5) An I-beam is assembled by three thin flat plates [26,27] and each of them is modeled as a Bernoulli-Euler beam with *thin rectangular section*.

2.1 Static and Kinematic Relations

Figure 1 shows a doubly symmetric I-beam composed of three thin plates. The centroidal axis of I-section coincides with the *x*-axis of the coordinate system, and *y* and *z* are the centroidal principal axes of the cross section. Let (u, v, w) and $(\theta_x, \theta_y, \theta_z)$ denote the centroidal displacements and rotations along the *x*-, *y*-, and *z*-axes of the I-beam at the position of *x*, respectively. According to the geometrical hypothesis of *rigid* cross section in assumption (3) for each of the sub-beams individually, the centroidal rotations of the sub-beams can be described as

$$\theta_{xT} = \theta_{xB} = \theta_{xw} = \theta_x, \tag{1}$$

$$\theta_{yw} = \theta_y = -w', \tag{2}$$

$$\theta_{zw} = \theta_z = v', \tag{3}$$

in which the subscript '*T*' denotes the top flange, '*B*' the bottom flange, and '*w*' the web. The prime means the differentiation with respect to coordinate axis *x*. Meanwhile, considering in-plane *rigid* section and a reasonably small twisting angle θ_x for a deformed I-beam, the transverse displacements at the centroid for each of the sub-beams in the displaced I-section (see Fig. 2) are given by [26,27]

$$v_T = v_B = v_w = v, \tag{4}$$

$$w_w = w, \tag{5}$$

$$w_T = w + \frac{h}{2}\theta_x, \tag{6}$$

$$w_B = w - \frac{h}{2}\theta_x, \tag{7}$$

in which $h \ (= d - t_f)$ means the distance between the centroid of two flanges of the symmetrical I-section. Meanwhile, the symbols shown in Fig. 2 are defined as: d = depth, b = width, t_f = flange thickness, and t_w = web thickness. From the assumption (5), the longitudinal displacements at the midpoints of the top flange, bottom flange, and web plate due to the bending rotation θ_z about the centroidal axis of the I-beam are respectively defined as (see Fig. 3):

$$u_T = u - \frac{h\theta_z}{2} = u - \frac{h}{2}v', \tag{8}$$

$$u_B = u + \frac{h\theta_z}{2} = u + \frac{h}{2}v', \tag{9}$$
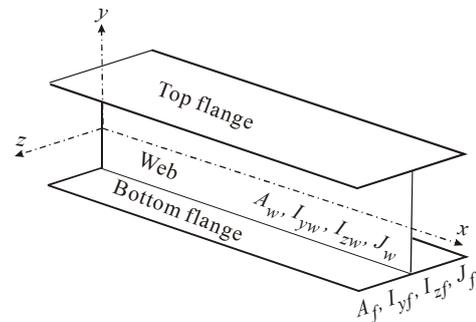
$$u_w = u. \tag{10}$$

Fig. 1 Coordinate system and formation of an I-beam

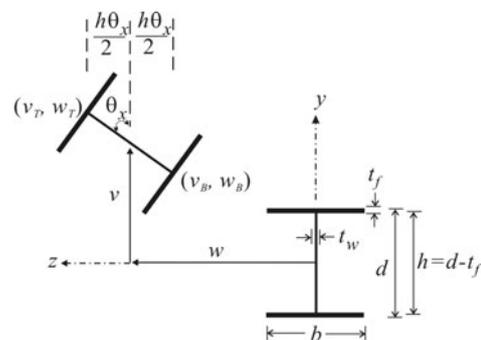
Fig. 2 Transverse displacements of a bi-symmetric I-section

As indicated in Eqs. (1)-(10), the portion of displacement components (u_T, u_B, v_T, v_B, w_T, w_B) in the flange sections can be expressed in terms of the centroidal displacements (u, v, w, θ_x, θ_y, θ_z) of a displaced I-section. Then the generalized stress-strain relationship for each of the thin plates can be derived using the assumption (3) of rigid I-section.

2.2 Generalized Stress-strain Relationships

As shown in Fig. 4, let us use the subscript "n" to denote the location of flat plates in a thin-walled I-beam, namely, $n = T$ means the top flange, $n = w$ the web plate, and $n = B$ the bottom flange. Considering the force components for each of the sub-beams dipicted in Fig. 4, the following notations are given: $^1F_{xn}$ = axial force, ($^1F_{yn}$, $^1F_{zn}$) = transverse shears, $^1M_{xn}$ = torque, and ($^1M_{yn}$, $^1M_{zn}$) = bending moments. And the superscript 1 denotes the initial (pre-buckling) configuration C_1 for the initial forces. By the Bernoulli-Euler beam theory of pure bending and the St. Venant's theory of uniform torsion for thin rectangular section [5], the internal forces are related to the generalized strains for the n-th sub-beam as follows

$$^1F_{xn} = EA_n u'_n = EA_n \left(u' - (y_n v')' \right), \tag{11}$$

$$^1M_{yn} = -EI_{yn} w''_n = -EI_{yn}(w + y_n \theta_x)'', \tag{12}$$

$$^1M_{zn} = EI_{zn} v'', \tag{13}$$

$$^1M_{xn} = GJ_n \theta'_x, \tag{14}$$

where

$$y_n = \begin{cases} h/2 & n = T, \text{ for top flange} \\ 0 & n = w, \text{ for web plate} \\ -h/2 & n = B, \text{ for bottom flange} \end{cases}, \tag{15}$$

and E and G = moduli of elasticity and shear, A_f = area of flange, A_w = area of web, I_{yf} = moment of inertia of flange about local y_f axis, I_{yw} = moment of inertia of web about local y_w axis, I_{zf} = moment of inertia of flange about local z_f axis, I_{zw} = moment of inertia of web about local z_w axis, J_f = torsional constant of flange, J_w = torsional constant of web. And the flexural shears acting on the nth sub-beam are given by [10]:

$$^1F_{yn} = -\frac{d\,^1M_{zn}}{dx}\Bigg|_{n=B,T,w}, \tag{16}$$

$$^1F_{zn} = \frac{d\,^1M_{yn}}{dx}\Bigg|_{n=B,T,w}. \tag{17}$$

With the aid of Eqs. (11)-(17), the full cross sectional forces (see Fig. 5) acting on the I-section at initial configuration C_1 can be obtained from the force resultants shown in Fig. 4:

$$^1F_x = \sum_{n=T,B,w} {}^1F_{xn} = EAu', \tag{18}$$

$$^1F_y = \sum_{n=T,B,w} {}^1F_{yn}, \tag{19}$$

$$^1F_z = \sum_{n=T,B,w} {}^1F_{zn}, \tag{20}$$

$$^1T_w = \left({}^1F_{zT} - {}^1F_{zB} \right)\frac{h}{2} = -EC_\omega \theta'''_x, \tag{21}$$

$$^1M_x = \left[\sum_{n=T,B,w} {}^1M_{xn} \right] + {}^1T_w = GJ\theta'_x - EC_\omega \theta'''_x, \tag{22}$$

$$^1M_y = \sum_{n=T,B,w} {}^1M_{yn} = -EI_y w'', \tag{23}$$

$$^1M_z = \left[\sum_{n=T,B,w} {}^1M_{zn} \right] + \left({}^1F_{xB} - {}^1F_{xT} \right)\frac{h}{2} = EI_z v'', \tag{24}$$

$$^1B_y = \left({}^1M_{yB} - {}^1M_{yT} \right)\frac{h}{2} = EC_\omega \theta''_x, \tag{25}$$
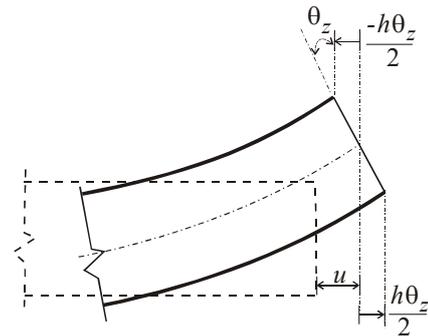
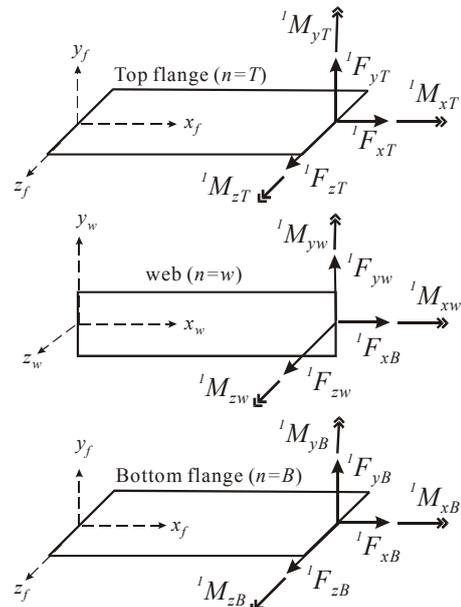Fig. 3 Plane section assumption of web plate for a deformed I-beam
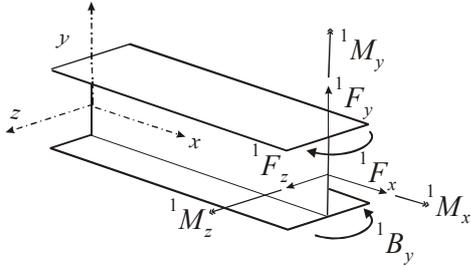
Fig. 4 Stress resultants on the sub-beams of an I-beam

Fig. 5 Cross sectional forces of an I-beam

were, ^1T_w = warping torque, and ^1B_y = bi-moment [3-5,26,27]. The sectional properties in Eqs. (18)-(25) are defined as: $A = 2A_f + A_w$ = area; $I_y = 2I_{yf} + I_{yw}$ = principle moment of inertia about the centroidal axis y; $I_z = 2I_{zf} + I_{zw} + A_f h^2/2$ = principle moment of inertia about the centroidal axis z; $J = 2J_f + J_w$ = torsional constant; and $C_\omega = I_{yf} h^2/2$ = warping constant. With the generalized stress-strain relationship given in Eqs. (18)-(25), one can relate the generalized strains to the full cross sectional forces on I-section as follows:

$$\begin{Bmatrix} u' \\ v'' \\ w'' \\ \theta_x' \\ \theta_x'' \end{Bmatrix} = \begin{bmatrix} 1/EA & 0 & 0 & 0 & 0 \\ 0 & 0 & 1/EI_z & 0 & 0 \\ 0 & -1/EI_y & 0 & 0 & 0 \\ 0 & 0 & 0 & 1/GJ & 0 \\ 0 & 0 & 0 & 0 & 1/EC_\omega \end{bmatrix} \begin{Bmatrix} ^1F_x \\ ^1M_y \\ ^1M_z \\ ^1T_{sv} \\ ^1B_y \end{Bmatrix}$$

(26)

where $^1T_{sv} = {}^1M_x - {}^1T_w$ = St. Venant torque. Thus the substitution of Eq. (26) into Eqs. (19)-(25) yields the following force components acting on the cross section of the n-th narrow beam in terms of full cross sectional forces of the I-beam:

$$^1F_{xn} = \frac{A_n}{A}{}^1F_x - \frac{A_f y_n}{2I_z}{}^1M_z,$$

(27)

$$^1M_{xn} = \frac{J_n}{J}{}^1T_{sv},$$

(28)

$$^1M_{yw} = \frac{I_{yw}}{I_y}{}^1M_y,$$

(29)

$$^1M_{yn} = \frac{I_{yn}}{I_y}{}^1M_y - \frac{^1B_y}{2y_n}\bigg|_{n=T,B},$$

(30)

$$^1M_{zn} = \frac{I_{zn}}{I_z}{}^1M_z,$$

(31)

$$^1F_{zw} = \frac{d\,^1M_{yw}}{dx} = \frac{I_{yw}}{I_y}{}^1F_z,$$

(32)

$$^1F_{zn} = \frac{d\,^1M_{yn}}{dx}\bigg|_{n=T,B} = \frac{I_{yn}}{I_y}{}^1F_z + \frac{^1T_w}{2y_n}\bigg|_{n=T,B},$$

(33)

$$^1F_{yn} = -\frac{d\,^1M_{zn}}{dx} = \frac{I_{zn}}{I_z}{}^1F_y.$$

(34)

With the relations of cross sectional force components shown in Eqs. (27)-(34) for each of sub-beams, the $[k_g]_{14 \times 14}$ matrix (including two nodal warping degrees of freedom) of a 3D I-beam element will be derived using rigid beam assemblage concept with the aids of Yang et al.'s simplified geometric stiffness matrix $[k_g]_{12 \times 12}$ [16] in the following section.

3. DERIVATION OF GEOMETRIC STIFFNESS MATRIX

The element stiffness equation of equilibrium for a spatial beam element in an updated Lagrangian form is [17]

$$[k_e]\{u\} + [k_g]\{u\} = \{^2f\} - \{^1f\}$$

(35)

where $[k_e]$ = elastic stiffness matrix, $[k_g]$ = geometric stiffness matrix, $\{u\}$ = element displacement vector, $\{^2f\}$ = the force vector referred to the displaced configuration C_2, and $\{^1f\}$ = the initial force vector applied at initial position C_1 (see Fig. 6).

Considering the kinematical relations of centroidal displacements in Eqs (1)-(10) and the 2-node I-beam element with 14 degrees of freedom (including nodal warping deformation at each node) in Fig. 7, the nodal displacement vector transformation between the n-th sub-beam element and the I-beam element is

$$\{\bar{\gamma}_n\}_{14 \times 1} = [T_n]_{14 \times 14}\{\gamma\}_{14 \times 1}$$

(36)
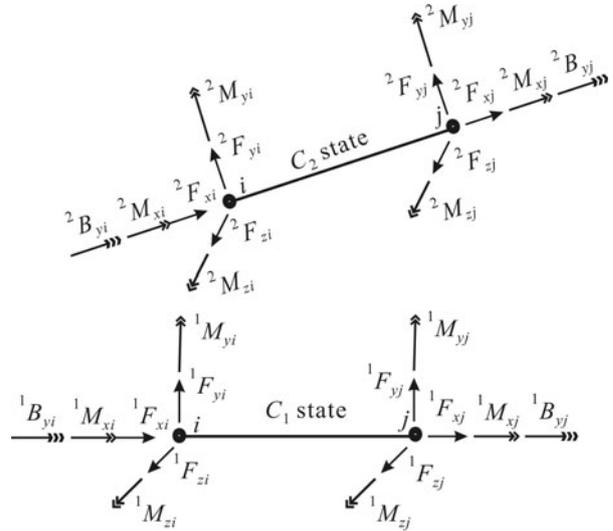

Fig. 6 Motion of a thin-walled beam element in space

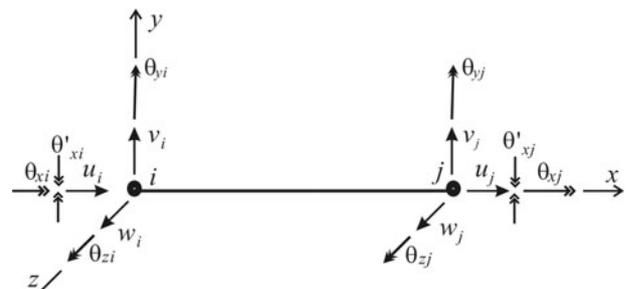Fig. 7 Nodal degrees of freedom of an I-beam element

where $\{\bar\gamma_n\}_{14\times1}$ = centroidal displacement vector of the n-th sub-beam element, $\{\gamma\}_{14\times1}$ = nodal displacement vector of the I-beam element, and

$$\{\bar\gamma_n\}_{14\times1} = \begin{Bmatrix} \langle u_n & v_n & w_n & \theta_{xn} & \theta_{yn} & \theta_{zn}\rangle_i^T \\ \langle u_n & v_n & w_n & \theta_{xn} & \theta_{yn} & \theta_{zn}\rangle_j^T \\ & & \langle 0 & 0 \rangle^T & & \end{Bmatrix}_{14\times1} \quad (37)$$

$$\{\gamma\}_{14\times1} = \begin{Bmatrix} \langle u & v & w & \theta_x & \theta_y & \theta_z\rangle_i^T \\ \langle u & v & w & \theta_x & \theta_y & \theta_z\rangle_j^T \\ & & \langle \theta'_{xi} & \theta'_{xj} \rangle^T & & \end{Bmatrix}_{14\times1} \quad (38)$$

As shown in Eq. (37), the null column vector $\langle 0 \quad 0\rangle^T$ represents the nodal warping deformations $\langle\theta'_{xi} \quad \theta'_{xj}\rangle^T$ vanish for the n-th sub-beam with *solid* section. The terms with θ'_x in Eq. (38) mean the nodal warping degrees of freedom. As for the transformation matrix $[T_n]_{14\times14}$, it is given as following

$$[T_n]_{14\times14} = \begin{bmatrix} [\iota_n]_{3\times3} & [t_{1n}]_{3\times3} & [0]_{3\times3} & [0]_{3\times3} & \{0\}_{3\times2} \\ [0]_{3\times3} & [\iota_n]_{3\times3} & [0]_{3\times3} & [0]_{3\times3} & \{t_{2n}\}_{3\times2} \\ [0]_{3\times3} & [0]_{3\times3} & [\iota_n]_{3\times3} & [t_{1n}]_{3\times3} & \{0\}_{3\times2} \\ [0]_{3\times3} & [0]_{3\times3} & [0]_{3\times3} & [\iota_n]_{3\times3} & \{t_{3n}\}_{3\times2} \\ \langle 0\rangle_{2\times3} & \langle 0\rangle_{2\times3} & \langle 0\rangle_{2\times3} & \langle 0\rangle_{2\times3} & [0]_{2\times2} \end{bmatrix}, \quad (39)$$

$$[\iota_n]_{3\times3} = \begin{bmatrix} 1 & 0 & 0 \\ 0 & 1 & 0 \\ 0 & 0 & 1 \end{bmatrix}, \quad (40)$$

$$[t_{1n}]_{3\times3} = y_n \begin{bmatrix} 0 & 0 & -1 \\ 0 & 0 & 0 \\ 1 & 0 & 0 \end{bmatrix}, \quad (41)$$

$$\{t_{2n}\}_{3\times2} = y_n \begin{Bmatrix} 0 & 0 \\ -1 & 0 \\ 0 & 0 \end{Bmatrix}, \quad (42)$$

$$\{t_{3n}\}_{3\times2} = y_n \begin{Bmatrix} 0 & 0 \\ 0 & -1 \\ 0 & 0 \end{Bmatrix}. \quad (43)$$

As a set of *self-equilibrium* nodal forces applying at a rigid beam element are subject to rigid body motions, the directions of the nodal forces will be changed but their magnitudes should remain the same for equilibrium. This is known as "rigid body motion rule" [16,17] for qualifying a derived geometric stiffness matrix. For this reason, let the I-beam element experience rigid body motions from C_1 to C_2, the elastic stiffness matrix $[k_e]$ of the stiffness equation in Eq. (35) simply vanishes [16,17]. Meanwhile, the warping-induced natural deformations of an I-beam would van-

ish as well. Because of this, only conventional six degrees of freedom (3 displacements + 3 rotations) at each node for the sub-beam element are considered. Thus the stiffness equation for the n-th sub-beam in the I-beam element becomes [16]

$$[k_{gn}]_{12\times12}\{\gamma_n\}_{12\times1} = \left(\{^2f_n\} - \{^1f_n\}\right)_{12\times1} \quad (44)$$

where $[k_{gn}]_{12\times12}$ = geometric stiffness matrix of the n-th sub-beam (3 translations and 3 rotations at each node), $\{^2f_n\}$ = force vector referred to the deformed configuration C_2, and $\{^1f_n\}$ = initial force vector applied at initial position C_1. For the sub-beam with solid section, Yang *et al.*'s rigid-body qualified $[k_g]_{12\times12}$ matrix [16] is available to represent the geometric stiffness matrix $[k_{gn}]_{12\times12}$ of the nth sub-beam, *i.e.*,

$$[k_{gn}]_{12\times12} = \begin{bmatrix} [g]_n & [h_i]_n & -[g]_n & [h_j]_n \\ [h_i]_n^T & [i_i]_n & -[h_i]_n^T & [0] \\ -[g]_n & -[h_i]_n & [g]_n & -[h_j]_n \\ [h_j]_n^T & [0] & -[h_j]_n^T & [i_j]_n \end{bmatrix}, \quad (45)$$

where the sub-matrices in Eq. (46) are given in Appendix I. It is noted that the St. Venant torque ($^1T_{svn}$) has been regarded as a semi-tangential (ST) torque and the bending moment as quasi-tangential (QT) moment in the sub-matrices $[i_i]_n$ and $[i_j]_n$ in Eq. (45). Thus the $[k_g]_{14\times14}$ matrix for a *rigid* I-beam element can be assembled through the following stiffness transformation [28]:

$$[k_g]_{14\times14} = \sum_{n=T,w,B} [T_n]_{14\times14}^T \begin{bmatrix} [k_{gn}]_{12\times12} & \{0\}_{2\times12} \\ \langle 0\rangle_{12\times2} & [0]_{2\times2} \end{bmatrix} [T_n]_{14\times14} \quad (46)$$

The geometric stiffness matrix $[k_g]_{14\times14}$ in Eq. (46) and its sub-matrices are given as follows:

$$[k_g]_{14\times14} = \begin{bmatrix} \begin{bmatrix} [G] & [H_i] & -[G] & [H_j] \\ [H_i]^T & [I_i] & -[H_i]^T & [0] \\ -[G] & -[H_i] & [G] & -[H_j] \\ [H_j]^T & [0] & -[H_j]^T & [I_j] \end{bmatrix}_{12\times12} & \{0\}_{12\times2} \\ \langle 0\rangle_{2\times12} & [0]_{2\times2} \end{bmatrix} \quad (47)$$

$$[G] = \frac{1}{L}\begin{bmatrix} 0 & -^1F_{y,j} & -^1F_{z,j} \\ -^1F_{y,j} & {}^1F_{x,j} & 0 \\ -^1F_{z,j} & 0 & {}^1F_{x,j} \end{bmatrix}, \quad (48)$$

$$[H_j] = \frac{1}{L}\begin{bmatrix} {}^1T_{w,j} & 0 & 0 \\ {}^1M_{y,j} & -^1T_{sv,j}/2 & 0 \\ {}^1M_{z,j} & 0 & -({}^1T_{sv,j}/2 + {}^1T_{w,j}) \end{bmatrix} \quad (49)$$

$$[I_j] = \begin{bmatrix} 0 & 0 & 0 \\ -^1M_{z,j} & 0 & {}^1T_{sv,j}/2 + {}^1T_{w,j} \\ {}^1M_{y,j} & -^1T_{sv,j}/2 & 0 \end{bmatrix}, \quad (50)$$

where L = length of the I-beam element. By replacing the terms ($^1T_{w,j}$, $^1T_{sv,j}$, $^1M_{y,j}$, $^1M_{z,j}$) in the sub-matrices $[H_j]$ and $[I_j]$ in Eqs. (49) and (50) by the terms ($^1T_{w,i}$, $^1T_{sv,i}$, $^1M_{y,i}$, $^1M_{z,i}$), one can obtain the sub-matrices $[H_i]$ and $[I_i]$ associated with end i of the I-beam element. As indicated in Eqs.(47)-(50), the rotational natures of bending and torsional moments have been taken into account, that is, the bending moments (^1M_y, M_z) and the warping torque (^1T_w) are treated as the QT moments and the St. Venant torque ($^1T_{sv}$) as the ST torque. This conclusion agrees very well with the nature of moments generated from the stress resultants acting on an I-section (see Fig. 8) for the St. Venant (T_{sv}) and warping (T_w) torques. Compare the geometric stiffness matrix $[k_g]_{14 \times 14}$ presented in Eq. (47) with the one $[k_g]_{14 \times 14}$ derived by Yang and McGuire [11,12], generally, the nodal forces of the corresponding equivalent terms in $[k_g]_{14 \times 14}$ nearly remain the same but the coefficients do not because the rigid-body qualified rule was applied to the present formulation. Meanwhile, the terms related to warping degrees of freedom become zero since the warping deformations are of natural deformation and they will not exist for an I-beam element undergoing rigid body motions. In addition, the nature of torsions and moments under rotations of I-section has been reasonably explained in the present $[k_g]_{14 \times 14}$ matrix. By neglecting the warping torque (^1T_w) and treating the St. Venant torque ($^1T_{sv}$) as the resistant torsion ^1M_x in Eqs. (49) and (50), the $[k_g]_{14 \times 14}$ matrix in Eq. (47) is reduced to Yang *et al.*'s rigid-body qualified geometric stiffness matrix [15] that the nature of applying torque is regarded as ST torque, which is denoted by $[k_g]_{\text{Yang}}$ in this study.

4. SOLUTION STRATEGY OF NONLINEAR ANALYSIS

To compute the nonlinear response of a loaded structure, the global stiffness equation for buckling/post-buckling analysis of the structure is expressed as the following incremental form [15-17]:

$$\left([K_e]+[K_g]\right)\{U\} = \{^2_1F\} - \{^1_1F\}. \qquad (51)$$

where $\{U\}$ = structural displacement increment vector from C_1 (initial state) to C_2 (current state). $[K_e]$ = structural elastic stiffness matrix, $[K_g]$ = structural geometric stiffness matrix, $\{^2_1F\}$ = applied force vector acting at the structure at C_2, and $\{^1_1F\}$ = applied force vector acting at the structure at C_1.

To trace the load-deflection response of geometrical nonlinear analysis from Eq. (51), the generalized displacement control (GDC) method proposed by Yang and Shieh [29] will be adopted for its general stability and reliability in dealing with multi loops and limit points in large-deflection analysis. In this study, the incremental-iteration procedure including three phases: *Predictor, corrector,* and *error-checking* [15-17, 32] is employed to compute the post-buckling response of framed structures with I-beams. The predictor phase

relates to the solution of structural displacement increments and the number of iterations at each incremental step. The corrector stage is concerned with recovery of internal forces for each element and it determines the accuracy of the element forces with reference to deformed state (configuration C_2). The error-checking phase deals with updating of the structural geometry and computes the unbalanced forces by deducting the internal resistant forces of structuers from the applied loads [10]. If the Euclid norms of unbalanced forces are greater than preset tolerances, another iteration involving the preceding three phases are carried out until the unbalanced forces are eliminated. Otherwise, go to the next increment.

5. NUMERICAL VERIFICATIONS

To examine the applicability of the proposed $[k_g]_{14 \times 14}$ matrix (see Eq. (47)) to thin-walled I-beam structures, the elastic stiffness matrix $[k_e]_{14 \times 14}$ of a tapered I-beam element given in reference [26], which can take the web-tapering effect of torsion into account [25], is employed to assemble the structural elastic stiffness matrix of an I-beam structure in this study. Besides, some benchmark buckling and post-buckling problems for simple structures composed of I-shaped beams will be carried out as well.

5.1. Lateral Buckling Analysis of Web-tapered I-beams

Figure 9 shows a simple beam with linearly web-tapered I-section, in which a central concentrated load P is acting above the top flange. This buckling problem was first investigated by Kitipornchai and Trahair [6] using equilibrium approach, in which induced warping constants of $I_{\omega\psi} = (2h'/h)C_\omega$ and $C_\psi = (2h'/h)^2 C_\omega$ for a web-tapered I-beam were derived and such new warping terms may affect torsional resistance of web-tapered I-beam structures against torsional-flexural buckling. Here C_ω means warping constant of a symmetrical I-section. It is noted that the induced torsional constant $I_{\omega\psi} = (2h'/h)C_\omega$ may reduce torsional resistance of a web-tapered I-beam if $h' < 0$ is considered. But the torsional resistance would be increased due to the induced torsional constant $C_\psi = (2h'/h)^2 C_\omega$. Because of this, a suitable adjustment of web-taper constant τ may result in the lateral buckling load appearing minimum. From numerical and experimental investigations, Kitipornchai and Trahair [6] further pointed out that there exists a minimum critical load for a linearly web-tapered I-beam as the web-tapering constant is close to 0.4. It means that the torsional resistance of the tapered-I beam would reach minimum near this critical web-tapering constant. With the elastic stiffness matrix of a tapered I-beam derived from reference [26], this example intends to compute the critical loads of a web-tapered I-beam with various web-taper constants to verify the validity of the present geometric stiffness.

For the purpose of illustration, the flange width *b*, flange thickness t_f, and web thickness t_w of the web-tapered I-beam are set to be constant. The dimensional properties of the web-tapered I-beam are referred to the paper presented in reference [6], in which the cross-sectional dimensions at the mid-span: b = 31.55mm, t_f = 3.11mm, h_0 = 72.76mm, t_w = 2.13mm, and τ = web-taper constant, and beam length L_0 = 1.52m. The material properties of elastic and shear moduli are E = 65.31GPa, G = 25.63GPa, respectively. Twenty tapered I-beam elements with the present $[k_g]_{14 \times 14}$ matrix are used to model the tapered I-beam. Let us define the web-tapering constant as $\tau = h/h_0$. Here h means the height at support end of the tapered I-beam. Eigen-value solutions for the elastic critical loads of the web-tapered I-beam have been performed and plotted against tapering constant in Fig. 10, in
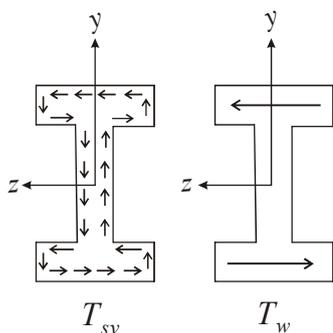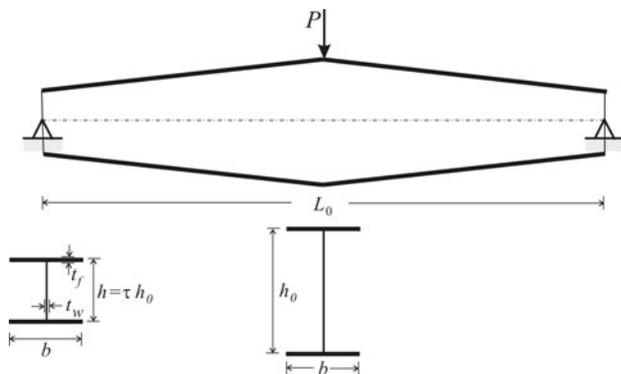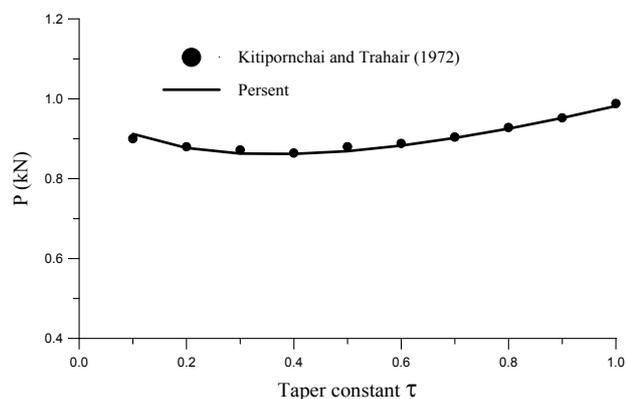
which the analytical results obtained by Kitipornchai and Trahair were shown [6]. From the response curve in Fig. 10, there exists a minimum value of buckling loads for the web-taper constant near 0.4. It means that the torsional resistance against lateral buckling for the web-tapered I-beam would become minimum at certain critical taper constant. Such a phenomenon was also observed in the theoretical and experimental work presented by Kitipornchai and Trahair [6].

5.2. Post-buckling Analysis of a Uniform Cantilever

A uniform I-shaped cantilever shown in Fig. 11 is subjected to a transverse load *P* and a small lateral imperfection load with 0.001P at its free end "B". The following material and geometric properties are adopted [24]: E = 2.06×10^8 kN/m^2, G = 7.92×10^6 kN/m^2, L = 10m, h = 0.613m, b = 0.19m, t_w = 0.025m, and t_f = 0.025m. The analytical result of lateral buckling load P_{cr} (= 47kN) can be obtained from the book written by Timoshenko and Gere [4]. To perform post-buckling analysis, twenty uniform I-beam elements with the present $[k_g]_{14 \times 14}$ matrix in Eq. (47) are used to model the cantilever I-beam. Figure 12 shows the load-deflection curves at the free end "B" obtained from the present predictions, which are in reasonable agreement with the numerical results given in references [19] and [24]. The discrepancies of the response curves can be attributed to the difference in the applied lateral imperfect point load at the free end "B". Since the present analysis has taken a small lateral imperfect load 0.001P into account, once the applying load *P* is beyond the lateral buckling load P_{cr}(= 47kN), the lateral displacement W_B at free end "B" increases significantly even with a small increase of *P*. It means the cantilever I-beam is situated in a post-buckled stage. Obviously, the feasibility and accuracy of the proposed $[k_g]_{14 \times 14}$ matrix is available for uniform I-beam elements in large-deformation response analysis.

Fig. 8   St. Venant torque (ST type) and warping torque (QT type).

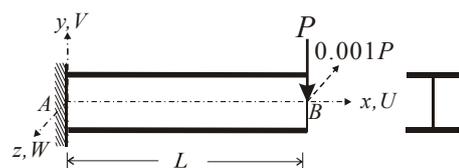Fig. 9   Linearly web-tapered I-beam with a central top flange load.

Fig. 11   Cantilever beam subjected to tip forces.

Fig. 10   Elastic critical loads of web-tapered I-beams.
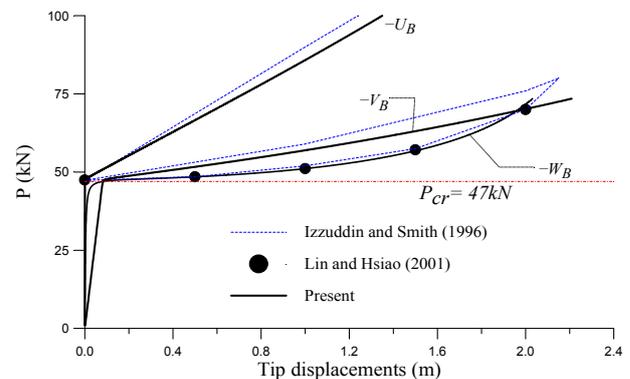

Fig. 12   Load-displacement curves for cantilever beam subjected to end force.

5.3 Geometrical Nonlinear Analysis of Right-angled Frames with Uniform I-section

As shown in Fig. 13, the geometric nonlinear analysis of a right-angled frame subjected to an in-plane load P at the free end was studied in references [19,26]. Let us consider the case that the fixed end **A** and corner junction **B** are warping prevented but the free end **C** is free to warp. An out-of-plane imperfection load p equal to one thousandth of P is applied at the free end (see Fig. 13). Let us adopt the same material and geometrical properties given in Section 5.2. Each member of the frame has a length of $L = 10$m and is modeled by 20 uniform I-beam elements. Considering the present $[k_g]_{14\times14}$ matrix, Fig. 14 shows the load-deflection curves of out-of-plane responses at the free end. It is seen that the present solution is reasonably close to the numerical predictions obtained from references [19,26]. Meanwhile, the proposed I-beam element has the ability to trace the post-buckling response of the right-angled frame even though the present $[k_g]_{14\times14}$ matrix is derived using the rigid beam assemblage concept.

5.4 Post-buckling Analysis of Simply Supported Beams with Web-tapered I-section

The same material and geometry data as those used in Example 5.1 are adopted. With the web-taper constant $= 0.5$, the tapered I-beam is subjected to the simultaneous action of a concentrated load P and an out-of-plane imperfection load p equal to one thousandth of P at the centroid of mid-span, as shown in Fig. 15(a). Twenty tapered I-beam elements with the present $[k_g]_{14\times14}$ matrix are used to model the tapered I-beam. To investigate the rotational effect of various
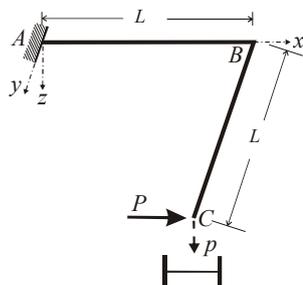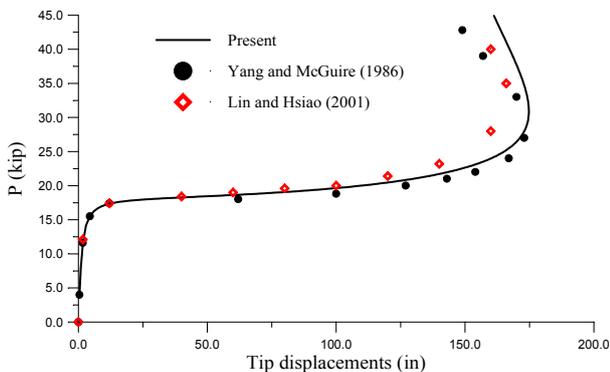
moments on the lateral post-buckling response of the web-tapered I-beam, Yang *et al.*'s simplified $[k_g]_{\text{Yang}}$ matrix [16] and the present $[k_g]_{14\times14}$ matrix (see Eq. (47)) are employed to analyze the same problem, respectively.

First, let us consider the case that the supports and mid-span of the web-tapered I-beam in Fig. 15(a) are of warping free. The load-deflection curves of out-of-plane displacement w_0 (see Fig. 15(b)) at mid-span are plotted in Fig. 16. The analysis results show that the post-buckling responses computed using the tapered I-beam element with either of $[k_g]_{14\times14}$ or $[k_g]_{\text{Yang}}$ are almost identical. The reason is that the uniform (ST) torque dominates the torsional resistance of the tapered I-beam with free warping supports.

Next, let us consider another case by restraining the warping deformations at the supports and mid-span of the tapered I-beam shown in Fig. 15(a). The load-deflection curves are also drawn in Fig. 16, as indicated, the warping restraint offers a significant resistance against torsional buckling strength and a discrepancy between the two response curves appears after the limit point **Q**, in which the tapered I-beam deforms by deflection and twist. As shown in Fig. 15(b), the centroidal load acting at the deformed I-beam will result in an additional torque (Pw_0), which is resisted by both of the warping and St. Venant torsions generated in the tapered I-beam. It means that the rotational property of warping torque (QT property) and St. Venant torque (ST property) plays an important role on the post-buckling response. For a twisted I-beam with warping restraints, its warping torsion would resist most of applied torques. This explains that the post-buckling response using the present $[k_g]_{14\times14}$ matrix (including QT warping torque and ST St. Venant torque) has less resistant capacity against the additional torque in comparison with the load-deflection curve computed by Yang *et al.*'s $[k_g]_{12\times12}$ matrix (including ST torque). It is concluded that if the warping torque were regarded as an ST torque for a tapered I-beam with warping restraint, the torsional resistance of the buckled I-beam structure would be overestimated. On the other hand, Fig. 17 depicts the warping deformations of the web-tapered I-beam with/without warping restraint supports at specific loads. It shows the warping deformation at mid-span is completely restrained due to symmetric property of structural deformations. Meanwhile, the present results indicate that for an

Fig. 13 Right angle frame subjected to tip forces.

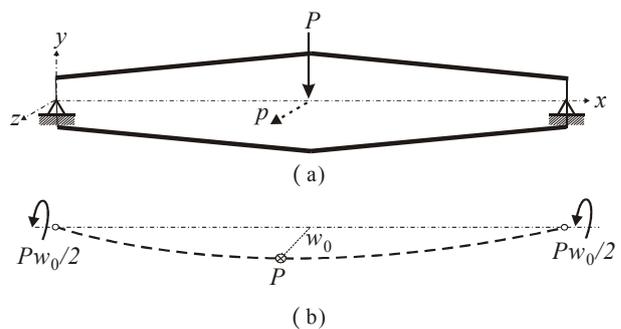Fig. 14 Load-displacement curve for cantilever angled frame.

Fig. 15 Web-tapered I-beam with a centroidal loading: (a) elevation; (b) plane on longitudinal axis.
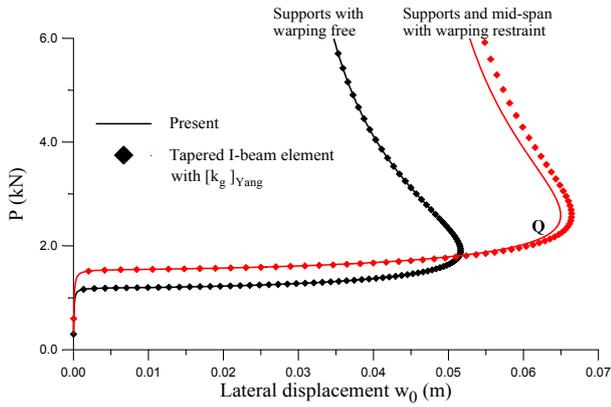
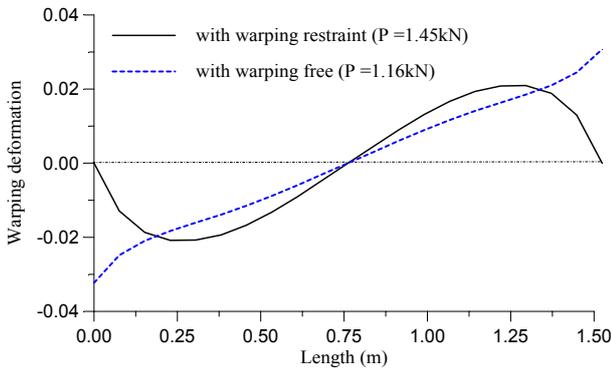Fig. 16 Load-deflection curves for web-tapered I-beam.

Fig. 17 Warping deformations of the web-tapered beam at specific loads

I-beam in torsional-flexural buckling stage, larger warping deformations would be induced for the I-beam with warping free even the applied load is smaller than the one with warping restraint. This is consistent with the physical phenomenon of a torsionally loaded I-beam.

6. CONCLUDING REMARKS

With Yang *et al.*'s rigid beam concept, this study adopts *rigid beam assemblage* concept in conjunction with stiffness transformation method to derive geometric stiffness matrix of a doubly symmetric I-beam element. Unlike conventional displacement-based finite element methods, the present element formulation is only concerned with the sub-sectional force components of an I-beam element in deriving the geometric stiffness matrix. Considering the rotational property of St. Venant torsion (ST type) and bending moment (QT type) for the sub-beam components in an I-beam element, the derived $[k_g]_{14 \times 14}$ matrix of an I-beam element can account for the induced moments of bending moments (QT type), warping torque (QT type), and St. Venant torque (ST type) under rotations. It is concluded that the induced moments of bending and twisting moments under rotations are related to the shape of cross section of thin-walled beams.

The numerical verifications indicate that the computed results of buckling and post-buckling analyses agree with those presented in existing literatures. According to the post-buckling response analysis of a tapered I-beam subject to a central load, the induced moments generated by the mechanism of resisting torques undergoing rotations play an important role in large deformations of loaded I-shaped beams. The load-deflection curves indicate that if the warping torque were regarded as an ST torque for a tapered I-beam with warping restraint, the torsional resistance of the buckled I-beam structure would be overestimated.

APPENDIX I

The sub-matrices of Yang *et al.*'s rigid body qualified geometric stiffness matrix [15-17] for a solid beam element about the centroidal axis of a tapered I-beam are:

$$[g]_n = \frac{1}{L}\begin{bmatrix} 0 & -^1F_{yn,j} & -^1F_{zn,j} \\ -^1F_{yn,j} & ^1F_{xn,j} & 0 \\ -^1F_{zn,j} & 0 & ^1F_{xn,j} \end{bmatrix}, \qquad (A.1)$$

$$[h_j]_n = \frac{1}{L}\begin{bmatrix} 0 & 0 & 0 \\ ^1M_{yn,j} & -^1T_{svn,j}/2 & 0 \\ ^1M_{zn,j} & 0 & -^1T_{svn,j}/2 \end{bmatrix}, \qquad (A.2)$$

$$[i_j]_n = \begin{bmatrix} 0 & 0 & 0 \\ -^1M_{zn,j} + {}^1F_{xn,j}y_n & 0 & ^1T_{svn,j}/2 + {}^1F_{zn,j}y_n \\ ^1M_{yn,j} & -^1T_{svn,j}/2 & 0 \end{bmatrix}.$$

$$(A.3)$$

Replacing the terms ($^1F_{xn,j}$, $^1F_{zn,j}$, $^1T_{svn,j}$, $^1M_{yn,j}$, $^1M_{zn,j}$) in the sub-matrices $[h_j]_n$ and $[i_j]_n$ by the terms ($-^1F_{xn,j}$, $-^1F_{zn,j}$, $^1T_{svn,i}$, $^1M_{yn,i}$, $^1M_{zn,i}$), one can obtain the sub-matrices $[h_i]_n$ and $[i_i]_n$ associated with end i.

REFERENCES

1. Johnston, B. G., "Lateral Buckling of I-section Columns with Eccentric Loads in Plane of Web," *Journal of Applied Mechanics*, **20**, p. 180 (1941).
2. Bleich, F., *Buckling Strength of Metal Structures*, McGraw-Hill, New York (1952).
3. Chen, W. F. and Atsuta, T., "Theory of Beam-Columns," **2**, *Space Behavior and Design*, McGraw-Hill, New York (1977).
4. Timoshenko, S. P. and Gere, J. M., *Theory of Elastic Stability*, 2nd Ed., McGraw-Hill, New York

(1961).

5. McGuire, W., *Steel Structures*, Prentice-Hall, New Jersey (1968).

6. Kitipornchai, S. and Trahair, N. S., "Elastic Stability of Tapered I-beams," *ASCE Journal of Structural Division*, **98**, pp. 713–728 (1972).

7. Kitipornchai, S. and Trahair, N. S., "Elastic Behavior of Tapered Monosymmetric I-beams," *ASCE Journal of Structural Division*, **101**, pp. 1661–1678 (1975).

8. Trahair, N. S., *Flexural-Torsional Buckling of Structures*, E & FN Spon, London, UK (1993).

9. Vlasov, V. Z., *Thin-Walled Elastic Beams*, 2nd Ed., Moscow, English translation, Jerusalem: Israel Program for Scientific Translation (1961).

10. Yang, Y. B. and Kuo, S. R., *Theory & Analysis of Nonlinear Framed Structures*, Prentice Hall, Singapore (1994).

11. Yang, Y. B. and McGuire, W., "Stiffness Matrix for Geometric Nonlinear Analysis," *ASCE Journal of Structural Engineering*, **112**, pp. 853–877 (1986).

12. Yang, Y. B. and McGuire, W., "Joint Rotation and Geometric Nonlinear Analysis," *ASCE Journal of Structural Engineering*, **112**, pp. 879–905 (1986).

13. Yang, Y. B. and Chiou, H. T., "Rigid Body Motion Test for Nonlinear Analysis with Beam Elements," *ASCE Journal of Engineering Mechanics*, **113**, pp. 1404–1419 (1987).

14. Yang, Y. B., Chang, J. T., and Yau, J. D., "A Simple Nonlinear Triangular Plate Element and Strategies of Computation for Nonlinear Analysis," *Computer Methods in Applied Mechanics and Engineering*, **178**, pp. 307–321 (1999).

15. Yang, Y. B., Kuo, S. R. and Wu, Y. S., "Incrementally Small-Deformation Theory for Nonlinear Analysis of Structural Frames," *Engineering Structures*, **24**, pp. 783–798 (2002).

16. Yang, Y. B., Lin, S. P. and Leu, L. J., "Solution Strategy and Rigid Element for Nonlinear Analysis of Elastic Structures Based on Updated Lagrangian Formulation," *Engineering Structures*, **29**, pp. 1189–1200 (2007).

17. Yang, Y. B., Lin, S. P. and Chen, C.S., "Rigid Body Concept for Geometric Nonlinear Analysis of 3D Frames, Plates and Shells Based on the Updated Lagrangian Formulation," *Computer Methods in Applied Mechanics and Engineering*, **196**, pp. 1178–1192 (2007).

18. Kwak, H. G., Kim, D. Y. and Lee, H. W., "Effect of Warping in Geometric Nonlinear Analysis of Spatial Beams," *Journal of Constructional Steel Research*, **57**, pp. 729–751 (2001).

19. Lin, W. Y. and Hsiao, K. M., "Co-Rotational Formulation for Geometric Nonlinear Analysis of Doubly Symmetric Thin-Walled Beams," *Computer Methods in Applied Mechanics and Engineering*, **190**, pp. 6023–6052 (2001).

20. Lin, W. Y. and Hsiao, K. M., "More General Expression for the Torsional Warping of a Thin-Walled Open Section Beam," *International Journal of Mechanical Science*, **45**, pp. 831–849 (2003).

21. Chen, H. H., Lin, W. Y. and Hsiao, K. M., "Co-Rotational Finite Element Formulation for Thin-Walled Beams with Generic Open Section," *Computer Methods in Applied Mechanics and Engineering*, **195**, pp. 2334–2370 (2006).

22. Chen, H. H. and Hsiao, K. M., "Coupled Axial–Torsional Vibration of Thin Walled Z-Section Beam Induced by Boundary Conditions," *Thin-Walled Structures*, **45**, pp. 573–583 (2007).

23. Chen, H. H. and Hsiao, K. M., "Quadruply Coupled Linear Free Vibrations of Thin-Walled Beams with Generic Open Section," *Engineering Structure*, **30**, pp. 1319–1334 (2008).

24. Yang, Y. B., Kuo, S. R. and Cherng, Y. D., "Curved Beam Elements for Nonlinear Analysis," *ASCE Journal of Engineering Mechanics*, **115**, pp. 840–855 (1989).

25. Yang, Y. B. and Yau, J. D., "Stability of Beams with Tapered I-sections," *ASCE Journal of Engineering Mechanics*, **113**, pp. 1337–1357 (1987).

26. Yau, J. D., "Stability of Tapered I-Beams Under Torsional Moments," *Finite Element Analysis and Design*, **42**, pp. 914–927 (2006).

27. Yau, J. D., "Elastic Stability of I-Columns Subjected to Compressions and Bi-moments," *Journal of Chinese Institute Engineers*, **30**, pp. 569–578 (2007).

28. McGuire, W. and Gallagher, R. H., *Matrix Structural Analysis*, John Wiley & Sons Inc., New York (1979).

29. Yang, Y. B. and Shieh, M. S., "Solution Method for Nonlinear Problems with Multiple Critical Points," *Journal of AIAA*, **28**, pp. 2110–2116 (1990).

30. Izzuddin, B. A. and Smith, D. L., "Large-Displacement Analysis of Elastoplastic Thin-Walled Frames. I: Formulation and Implementation," *Journal of Structural Engineering*, ASCE, **122**, pp. 905–914 (1996).

31. Izzuddin, B. A. and Smith, D. L., "Large-Displacement Analysis of Elastoplastic Thin-Walled Frames. II: Verification and Application," *ASCE Journal of Structural Engineering*, **122**, pp. 915–925 (1996).

32. Yau, J. D., "An Iterative Approach for Linear Torsion Analysis of Web-tapered I-Beams Using Uniform I-beam Element," *International Journal of Structural Stability and Dynamics*, **8**, pp. 521–529 (2008).

33. Andrade, A. and Camotim, D., "Lateral–Torsional Buckling of Singly Symmetric Tapered Beams: Theory and Applications," *ASCE Journal of Engineering Mechanics*, **131**, pp. 586–597 (2005).